**Journal of Hydraulic Structures**
*J. Hydraul. Struct.*, 2019; 5(2):32-48
**DOI: 10.22055/jhs.2019.29402.1107**

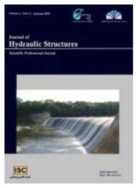

OPEN ACCESS

# Transient Measurement Site Design in Pipe Networks Using the Decision Table Method (DTM)

Mohammad Hadi Ranginkaman[1]
Amir Houshang Ayati[2]
Amin Ebrahim Bakhshipour[3]
Ali Haghighi[4]

## Abstract

The accuracy of leak detection and calibration of pipe networks by means of the inverse transient analysis (ITA) is highly affected by the number and location of the measurement sites. This study introduces a conceptual decision-making model, the Decision Table Method (DTM), for measurement site design of pipe networks with the aim of inverse transient analysis. Through the Decision Table Method, near optimum measurement sites are decided based on two criteria of the maximum sensitivity of measurement sites and the maximum diversity of sensitivity with respect to unknown parameters of leak areas and friction factors. The main advantage of DTM is that even in case of large networks, calculation of the Hessian matrix and the utilization of any optimization algorithm are not required. To evaluate the efficiency and applicability of the method, it is applied on two pipe networks of small and large size from the literature and the results are compared with the previous methods. Accordingly, the DTM is found reliable as well as easy to understand and implement.

**Keywords:** Inverse Transient Analysis (ITA), Measurement site design, Decision making, Leak detection, Calibration.

Received: 5 June 2019; Accepted: 6 September 2019

---

[1] Department of Civil Engineering, Shahid Chamran University of Ahvaz, Ahvaz, Iran . ha.ranginkaman@gmail.com
[2] Department of Civil Engineering, Shahid Chamran University of Ahvaz, Ahvaz, Iran, Saha.science@gmail.com **(Corresponding author)**
[3] University of Stuttgart, Institute for Sanitary Engineering, Water Quality and Solid Waste Management, Stuttgart, Germany. Amin.bakhshipour@gmail.com
[4] Department of Civil Engineering, Shahid Chamran University of Ahvaz, Ahvaz, Iran, A.haghighi@scu.ac.ir.

## 1. Introduction

The inverse transient analysis (ITA) is a renowned model-based approach for leak detection and calibration in piping systems. The ITA process includes estimations of two sets of unknown parameters, leak areas and pipe friction factors, through the minimization of the differences between observed and model-predicted values of the transient heads at the measurement sites. To solve this optimization problem, a nonlinear optimization solver is coupled with a transient simulation model to minimize the objective function (e.g., least squares errors). At this scheme, the intensity of transient head variation depends on the location of measurement site; therefore, nodes with higher sensitivity of transient head to the unknowns play a prominent role in determining leaks and pipe friction factors, and the data acquisition from more sensitive nodes could enhance the authenticity of the ITA results. In fact, higher sensitivity of the objective function to the unknowns leads to significant gradients in the ITA's search space and makes it more convex. Hence, the number and location of measurement sites as optimization variables in sampling design problem is a key factor in the ITA success.

Generally, the optimum measurement sites design is defined by developing some approaches and criteria to select a set of flow and pressure heads sampling sites from all possible combinations of candidate nodes. Such a procedure, by nature, is a discrete multi-criteria decision-making problem. Considering a certain number of measurement sites, there exist a large number of combinations for allocating the sites in the network. Therefore, proper criteria are required to evaluate the merits of each measurement site design for solving the ITA reliably.

Historically, the field of groundwater monitoring has a significant contribution in developing the optimal site design approaches [1-13]. In the field of inverse transient analysis, several investigations have been performed to address the measurements and sampling site design issue in pipe networks and leak detection. In general, there exist two approaches to solve the optimal measurement sites problem based on various indices, criteria, and objective functions. The first is the full enumeration and the second is optimization. In the full enumeration method, all possible combinations of measurement sites in the network are evaluated and then the best decisions are made based on the considered fitness criterion. However, in large-scale problems, the full enumeration approach is computationally burdensome and time-consuming. In the case of large systems, applying an optimization model can solve the problem more efficiently. Over the past three decades, several investigations concerning measurement site design in the field of ITA have been conducted [14].

Liggett and Chen [15] suggested that the measurement sites should be in places with the highest sensitivity to the unknown parameters, leakage and pipe friction factors. Accordingly, they introduced two sensitivity indices based on the rate of success in solving the inverse problem and the sensitivity of the measurements to unknown parameters. In that study, they apply a variant of the Levenberg-Marquardt method (Press et al. 1986) to minimize the ITA objective function.

Vitkovsky et al. [14] dealt with the optimal design of measurement sites in the ITA problems. They introduced three indices which the first one ($\eta_j$) was defined based on the Jacobean matrix of pressure heads in candidate locations and the second and third indices ($\eta_A$ and $\eta_D$) was to evaluate the performance of the ITA with regard to possible errors associated with the problem's parameters. In that study, three optimization problems were governed and the genetic algorithm were utilized to find the optimum number of measurement sites.

Shamloo and Haghighi [16] introduced a method for optimal determination of measurement sites in leak detection and calibration of pipe networks through ITA. Their method was based on a ranking approach and used the Jacobian matrix of transient pressure heads with respect to the

ITA unknowns. They applied sequential quadratic programming (SQP) for optimization purposes.

Gamboa and Reis [17] took the advantage of NSGA-II for sampling design of pipe networks in leak detection. They introduced a set of four criteria to reach a proper sampling design. The first two criteria of (1) total leak sensitivity and (2) sensitivity consistency were to be maximized and the second two measures of (3) information redundancy and (4) sensors number were to be minimized. A hydraulic simulation model was used for sensitivity analysis and the consistency of sensitivity to all supposed leaks was estimated by entropy.

Despite all the advantages of the existing approaches for measurement sites design, a number of disadvantages could be considered especially in case of implementation in large networks. Some of these noticeable shortcomings are as the following:

1. The need for the high volume of computational efforts.
2. The necessity for defining mathematical programming and application of the optimization algorithm to achieve the optimum combination of measurement sites.
3. Due to the largeness of the problem, population-based algorithms such as GA that is stochastic by nature, could not guarantee to achieve a global optimum. Additionally, running the optimization algorithm for several times through different seeds, which is inevitable to find a suitable response, could end up in higher computational cost [15]
4. The possibility of inexistence value for some indices.
5. The poor scattering of the measurement sites.

To address the aforementioned issues, a novel conceptual decision-making model, the Decision Table Method (DTM), is introduced in the present study. The DTM procedure is based on the ranking system respecting the sensitivity of candidate nodes to the unknown parameters and spatial diversification of them in the network domain. In the following sections, the proposed algorithm is described as a step-by-step procedure and an illustrative flowchart. Then, the performance of the model is assessed using two demonstrative cases from the literature; a small and a large water distribution network. Finally, the results are compared with the previous methods and the advantages and disadvantages of the DTM are discussed.

## 2. Problem Formulation

The inverse problem for leak detection and calibration is presented in Eq. 1.

$$[\boldsymbol{A} \quad \boldsymbol{f}] = \emptyset(h\_ij) \quad i = 1 \ to \ M \quad and \quad j = 1 \ to \ NS \tag{1}$$

In which $A$ is the vector of the unknown parameters of leak areas, $f$ is the vector of the unknown parameters of pipe friction factors, $h_{ij}$ is the transient head at node $j$ at time step $i$, $M$ is the number of transient modeling time step and $NS$ = the number of (possible) candidate nodes as a location for pressure measurement.

The transient head in the selected measurement sites must be more sensitive to all unknown parameters compared with the other candidates. The measurement sites with low transient head sensitivity could not depict the effects of the unknown parameters variation appropriately. Therefore, there could exist a variety of responses for each parameter that satisfy the convergence condition of the ITA problem. In this paper, transient sensitivities of the measurement sites are obtained by the pressure head's partial derivations in each site with respect to unknown parameters of leak areas and friction factors as:

$$S_{A_{kj}} = \sum_{i=1}^{M} \left| \frac{\partial h_{ij}}{\partial A_k} \right| \quad k = 1 \; to \; NL \; and \; j = 1 \; to \; NS \tag{2}$$

$$S_{f_{lj}} = \sum_{i=1}^{M} \left| \frac{\partial h_{ij}}{\partial f_l} \right| \quad l = 1 \; to \; NP \; and \; j = 1 \; to \; NS \tag{3}$$

In which $S_{A_{kj}}$ and $S_{f_{lj}}$ are, respectively, the pressure sensitivity of site $j$ with respect to leak area $A_k$ at node $k$ and the pipe friction factor $f_l$ of pipe l, $NS$ is the number of (possible) candidate measurement sites, $NL$ is the number of leaks, $NP$ is the number of pipes. To calculate the elements of the above two mentioned matrices, a numerical model of transient flow analysis is implemented. At first, a mathematical model for the network is configured. Thereafter, the values of leak areas assumed to be zero in all main nodes. Then, the pipe friction factors are defined considering pipe material, network age and engineering judgement. Such a condition could be dealt as a basic status of the model. Afterwards, based on the network basic condition, the elements of the above matrices are calculated for each candidate site $j$ applying equations (2) and (3). To do so, simple finite difference estimation is used for discretization and numerical solution of the equations as follows:

$$S_{A_{kj}} = \sum_{i=1}^{M} \left| \frac{h_{ij}(A_k + \Delta A) - h_{ij}(A_k)}{\Delta Ae} \right| \quad k = 1 \; to \; NL \; and \; j = 1 \; to \; NS \tag{4}$$

$$S_{f_{lj}} = \sum_{i=1}^{M} \left| \frac{h_{ij}(f_k + \Delta f) - h_{kj}(f_k)}{\Delta f} \right| \quad l = 1 \; to \; NP \; and \; j = 1 \; to \; NS \tag{5}$$

In these equations, $\Delta A$ and $\Delta f$ are the partial differentiates of the leak area and pipe friction factor, respectively, which are added to each parameter in order to calculate the numerical values of $\boldsymbol{S_A}$ and $\boldsymbol{S_f}$ matrices.

## 3. Decision Table Model

The DTM based approach for measurement site design is performed according to the following steps:

1. The numerical values of $\boldsymbol{S_A}$ and $\boldsymbol{S_f}$ matrices are calculated using Eq.4 and Eq.5. Then, each row of these matrices is ranked according to the sensitivity and then is saved in two matrices named $\boldsymbol{Rank_A}$ and $\boldsymbol{Rank_f}$, in the way that the rank equal to 1 and NS are allocated to elements with the highest sensitivity and the lowest sensitivity, respectively. In fact, each row of these matrices represents the effects of leak areas or pipe friction factors in each candidate measurement site. It is worth mentioning that the derivation matrices corresponding leak areas and pipe friction factors are studied separately here.
2. The summation of ranks in each node is saved in two vectors namely $\boldsymbol{Sum_A}$ and $\boldsymbol{Sum_f}$ that indicate the sum of ranks in each candidate node with respect to leak areas and pipe friction factor, respectively.

$$Sum_{A_j} = \sum_{i=1}^{NL} Rank_{A_{ij}} \qquad j = 1 \; to \; NS \tag{6}$$

$$Sum_{f_j} = \sum_{i=1}^{NP} Rank_{f_{ij}} \qquad j = 1\ to\ NS \tag{7}$$

3. In $\boldsymbol{Rank_A}$ and $\boldsymbol{Rank_f}$ matrices, the node with the lowest value of rank summation is selected as the measurement site. It means that, this node has the highest priority compared to others.
4. In $\boldsymbol{Rank_A}$ and $\boldsymbol{Rank_f}$, all elements in rows with the rank number smaller or equal to the rank of latest selected site (in step 3) is substituted with zero. Through this substitution, the effect of $Sum_{A_j}$ and $Sum_{f_j}$parameters will be eliminated in the future selections, because the selected nodes in step 3 possess the best priority according to these parameters .
5. If all elements of $\boldsymbol{Rank_A}$ and $\boldsymbol{Rank_f}$ change into zero in step 4, the algorithm goes to step 6; otherwise, the vectors $\boldsymbol{Sum_A}$ and $\boldsymbol{Sum_A}$ are calculated using new values from step 4 and then the algorithm returns to step 3.
6. When all elements of Rank matrix turn into zero, the columns that correspond to all already selected nodes are changed to zero and the new rank matrix is applied for the rest of procedure and the algorithm returned to step 2.
7. The algorithm stops provided that all nodes are selected. Nodes acquire the higher priority according to the order of their selection. It means that to choose $NS$ nodes from the whole $NTS$ candidate node, simply, the first $NS$ node should be picked from the decision table. For more clarification, Figure (1) illustrates the decision table method in flowchart form.

In DTM, the determination of the priority of sites with respect to leak and pipe friction factors performs in separate procedures and eventually, the final decision is made through the integration of the results. Furthermore, due to the application of the Jacobian Matrix in determining the sensitivity, high priority site parameters are eliminated in order to maintain the dispersion ratio.

## 4. Application of the DTM to Network Examples

In order to study the performance of the DTM, two small and large networks from the literature [15] are considered here as case studies.

### Example 1: Small Network

The first example (Figure 2) is initially introduced by [14]. This network includes 11 pipes ($NP = 11$), 7 nodes ($NL = NS = 6$). A reservoir with a constant head of 30 m is located in node 1 and a constant inflow of 20 $lit/s$ in node 7 feeds the network. All pipes share a common diameter of $254mm$, a common length of $762m$ and a common wave speed of $1316\ m/s$. Leaks are assumed to occur at the nodes except at the reservoir. In this case, only leak areas were considered as the unknown parameters of the problem. To produce the transient flow, a valve located at node 4 was partially closed at a time of 2.0 seconds reducing the initial outflow from 58 $L/s$ to 28 $L/s$ in a linear fashion in 10 seconds then opened restoring the flow to 58 $L/s$ in another 10 second. Figure 3 shows the variations in head during transient at all measurement site candidates.

Firstly, according to the DTM flowchart, the $\boldsymbol{S_A}$ matrix of leak areas is calculated utilizing the transient flow analysis model based on the Method of Characteristics (MOC). The results from this stage are presented in Table 1. At the next stage, the $S_A$ matrix rows were ranked according to sensitivity. (Table 2).

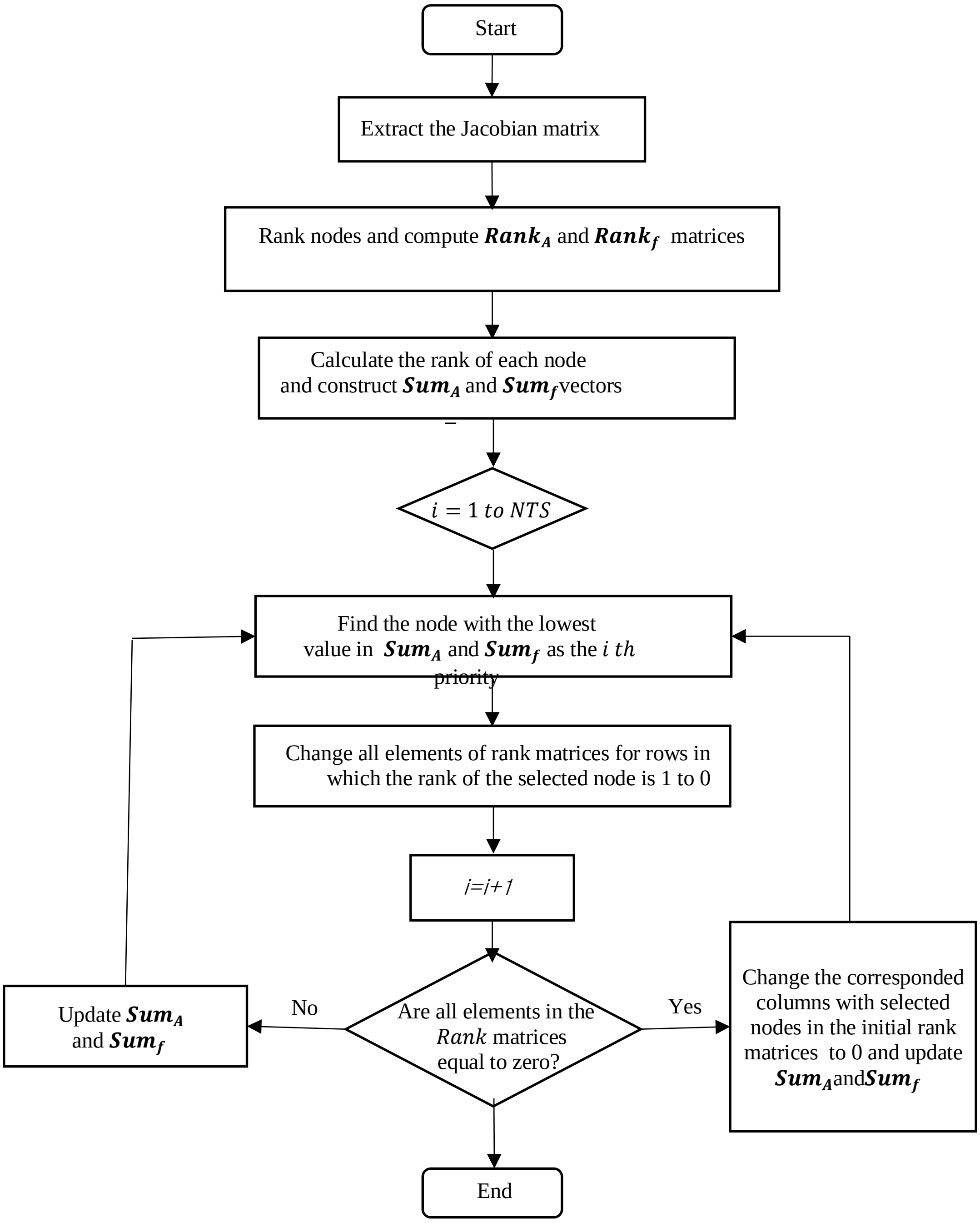


**Figure 1. The DTM flowchart**

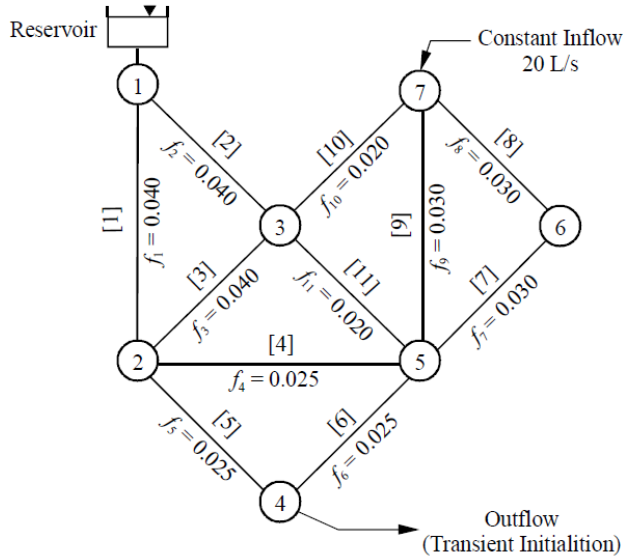


**Figure 2. Example 1 water distribution network**

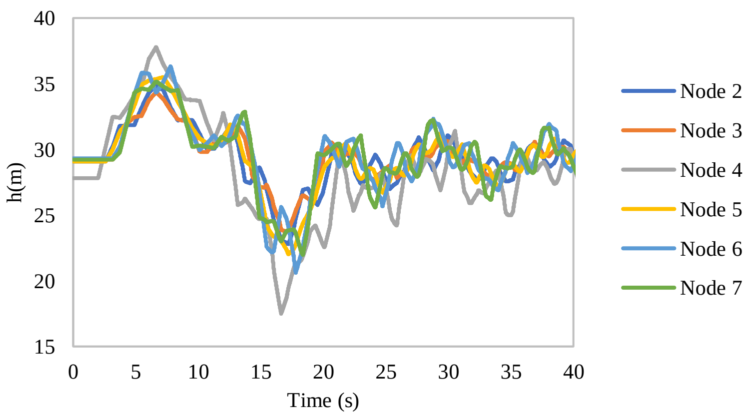


**Figure 3. Pressure variations in nodes of Example 1 due to excitation**

**Table 1. Jacobian matrix of pressures to the leak area (Example 1) ($^{\text{meters}}/_{\text{cm}^2}$)**

| Leak location | Pressure measurement sites | | | | | |
|---|---|---|---|---|---|---|
| | Node2 | Node3 | Node4 | Node5 | Node6 | Node7 |
| Node 2 | 5.39E+03 | 4.26E+03 | 6.67E+03 | 5.58E+03 | 6.43E+03 | 5.82E+03 |
| Node 3 | 4.22E+03 | 5.44E+03 | 5.60E+03 | 5.59E+03 | 6.54E+03 | 5.79E+03 |
| Node 4 | 6.27E+03 | 5.91E+03 | 8.91E+03 | 6.75E+03 | 8.60E+03 | 7.13E+03 |
| Node 5 | 5.25E+03 | 5.39E+03 | 6.62E+03 | 7.16E+03 | 7.68E+03 | 7.19E+03 |
| Node 6 | 6.14E+03 | 6.45E+03 | 9.13E+03 | 7.42E+03 | 1.01E+04 | 8.32E+03 |
| Node 7 | 5.68E+03 | 5.46E+03 | 7.29E+03 | 7.03E+03 | 8.58E+03 | 8.90E+03 |

**Table 2. Sensitivity ranking of the Jacobian matrix rows (Example 1)**

| | Pressure measurement sites | | | | | |
|---|---|---|---|---|---|---|
| Leak location | Node2 | Node3 | Node4 | Node5 | Node6 | Node7 |
| Node 2 | 5 | 6 | 1 | 4 | 2 | 3 |
| Node 3 | 6 | 5 | 3 | 4 | 1 | 2 |
| Node 4 | 5 | 6 | 1 | 4 | 2 | 3 |
| Node 5 | 6 | 5 | 4 | 3 | 1 | 2 |
| Node 6 | 6 | 5 | 2 | 4 | 1 | 3 |
| Node 7 | 5 | 6 | 3 | 4 | 2 | 1 |
| $\boldsymbol{Sum_A}$ | 33 | 33 | 14 | 23 | 9 | 14 |

The node with the lowest summation rank value (here is the node 6) is chosen as the first selected measurement site. Then, the elements of the corresponding rows with the rank equal to 1 for the selected measurement site, is substituted with zero. The reason for this substitution stems from the fact that, the previously mentioned unknowns have a representative in selected measurement sites, and therefore it is necessary to give other nodes a chance to be selected. According to data from the Table 3, node 6 could be considered as the first priority for the unknown parameter of leak area at nodes 3, 5 and 6. Therefore, all members of leak matrix should change into zero. Consequently, the decision table is updated respecting the data from the Table 3.

**Table 3. Updating all elements in rows which the rank of their selected node is equal to one (Example 1)**

| | Pressure measurement sites | | | | | |
|---|---|---|---|---|---|---|
| Leak location | Node2 | Node3 | Node4 | Node5 | Node6 | Node7 |
| Node 2 | 5 | 6 | 1 | 4 | 2 | 3 |
| Node 3 | 0 | 0 | 0 | 0 | 0 | 0 |
| Node 4 | 5 | 6 | 1 | 4 | 2 | 3 |
| Node 5 | 0 | 0 | 0 | 0 | 0 | 0 |
| Node 6 | 0 | 0 | 0 | 0 | 0 | 0 |
| Node 7 | 5 | 6 | 3 | 4 | 2 | 1 |
| $\boldsymbol{Sum_A}$ | 15 | 18 | 5 | 12 | 6 | 7 |

As the next step, $\boldsymbol{Sum_A}$ is recalculated and node 4 is chosen as the second node of the selected measurement site. Afterwards, all members of the rows in which the node 4 is their first priority (Node2, Node 4) substitutes with zero and the summation of the nodes ranks is recalculated.

According to the data from Table 4, node 7 is picked as the third priority to locate a sensor. Here, by turning the rows for which node 3 is the first priority into zero (row 7), the matrix will turn into a zero matrix. It means that all unknowns have a representative node in the selected sites. Thereafter, the columns which correspond to already selected sites (nodes 4,6,7) are eliminated in the initial rank matrix and a new rank matrix is achieved according to table 5. On this basis, to determine the next priority of the measurement site, computations are repeated utilizing the new rank matrix.

**Table 4. Calculating the rank summation of the nodes in the updated matrix (Example 1)**

| | Pressure measurement sites | | | | | |
|---|---|---|---|---|---|---|
| Leak location | Node2 | Node3 | Node4 | Node5 | Node6 | Node7 |
| Node 2 | 0 | 0 | 0 | 0 | 0 | 0 |
| Node 3 | 0 | 0 | 0 | 0 | 0 | 0 |
| Node 4 | 0 | 0 | 0 | 0 | 0 | 0 |
| Node 5 | 0 | 0 | 0 | 0 | 0 | 0 |
| Node 6 | 0 | 0 | 0 | 0 | 0 | 0 |
| Node 7 | 5 | 6 | 3 | 4 | 2 | 1 |
| $\boldsymbol{Sum_A}$ | 5 | 6 | 3 | 4 | 2 | 1 |

**Table 5. Calculating the rank summation of the candidate nodes that remain after elimination of the columns corresponding to selected nodes (Example 1)**

| | Pressure measurement sites | | |
|---|---|---|---|
| Leak location | Node2 | Node3 | Node5 |
| Node 2 | 5 | 6 | 4 |
| Node 3 | 6 | 5 | 4 |
| Node 4 | 5 | 6 | 4 |
| Node 5 | 6 | 5 | 3 |
| Node 6 | 6 | 5 | 4 |
| Node 7 | 5 | 6 | 4 |
| $\boldsymbol{Sum_A}$ | 33 | 33 | 23 |

Regarding the values from Table 5, node 5 is selected as the fourth measurement site priority. After this, because node 5 does not possess rank 1 or 2, the rows correspond to the parameters for which owned the rank 3 (node 5) turn into zero and the value of $\boldsymbol{Sum_A}$ is updated. As a result, Table 6 is achieved based on which, node 2 should be picked as the fifth priority. In this condition, the only remained node is node 3 which is the final measurement site priority.

Eventually, the best configuration of measurement site considering the number of sites is presented in Table 7. To evaluate the DTM, the results are compared to ones from [14] in Tables 8 to 10. In each table, various layouts of the measurement site from both methods are presented together with data from the calculation of $\eta_j$ , $\eta_A$ or $\eta_D$ indices. Comprehensive description of theses indices is presented in [14]. Comparison of the results shows that the DTM is able to perform measurement site design with close results to ones from [14].

**Table 6. Calculation of the summation of nodes which are remained after changing the row 5 elements to zero (Example 1)**

| | Pressure measurement sites | | |
|---|---|---|---|
| Leak location | Node2 | Node5 | Node7 |
| Node 2 | 5 | 6 | 4 |
| Node 3 | 6 | 5 | 4 |
| Node 4 | 5 | 6 | 4 |
| Node 5 | 0 | 0 | 0 |
| Node 6 | 6 | 5 | 4 |
| Node 7 | 5 | 6 | 4 |
| $\boldsymbol{Sum_A}$ | 27 | 28 | 20 |

**Table 7. The optimum configuration of Example 1 for leak detection**

| $N_S$ | Best measurement site configuration |
|---|---|
| 1 | 6 |
| 2 | 4,6 |
| 3 | 4,6,7 |
| 4 | 4,5,6,7 |
| 5 | 2,4,5,6,7 |
| 6 | 2,3,4,5,6,7 |

**Table 8. Comparison of DTM results with those from [14] based on $\eta_j$ (Example 1)**

| $N_S$ | DTM | $\eta_J$ | Vitkovsky et.al 2003[15] | $\eta_J$ |
|---|---|---|---|---|
| 1 | 6 | 4.80E+04 | 6 | 4.80E+04 |
| 2 | 4,6 | 9.22E+04 | 6,7 | 9.11E+04 |
| 3 | 4,6,7 | 1.35E+05 | 4,6,7 | 1.35E+05 |
| 4 | 4,5,6,7 | 1.75E+05 | 4,5,6,7 | 1.75E+05 |
| 5 | 2,4,5,6,7 | 2.08E+05 | 2,4,5,6,7 | 2.08E+05 |
| 6 | 2,3,4,5,6,7 | 2.41E+05 | 2,3,4,5,6,7 | 2.41E+05 |

**Table 9. Comparison of DTM results with those from [14] based on $\eta_D$ (Example 1)**

| $N_S$ | DTM | $\eta_D$ | Vitkovsky et.al 2003[14] | $\eta_D$ |
|---|---|---|---|---|
| 1 | 6 | 2.60E+21 | 4 | 2.50E+21 |
| 2 | 4,6 | 2.10E+23 | 4,6 | 2.10E+23 |
| 3 | 4,6,7 | 1.16E+24 | 4,6,7 | 1.16E+24 |
| 4 | 4,5,6,7 | 2.91E+24 | 3,4,6,7 | 3.53E+24 |
| 5 | 2,4,5,6,7 | 7.58E+24 | 3,4,5,6,7 | 7.76E+24 |
| 6 | 2,3,4,5,6,7 | 1.85E+25 | 2,3,4,5,6,7 | 1.85E+25 |

**Table 10. Comparison of DTM results with those from [14] based on $\eta_A$ (Example 1)**

| $N_S$ | DTM | $\eta_A$ | Vitkovsky et.al 2003[14] | $\eta_A$ |
|---|---|---|---|---|
| 1 | 6 | 2.71E-03 | 4 | 2.68E-03 |
| 2 | 4,6 | 1.23E-03 | 4,6 | 1.23E-03 |
| 3 | 4,6,7 | 9.57E-04 | 3,4,6 | 9.78E-04 |
| 4 | 4,5,6,7 | 8.03E-04 | 3,4,6,7 | 7.77E-04 |
| 5 | 2,4,5,6,7 | 6.73E-04 | 2,3,4,6,7 | 6.30E-04 |
| 6 | 2,3,4,5,6,7 | 5.61E-04 | 2,3,4,5,6,7 | 5.61E-04 |

## Example 2: Large Network

At this point, to evaluate the DTM in face of large networks, the network (Figure 4) originally introduced by [18] is utilized. This network includes 51 pipes (NP=51) and 35 nodes (NL=34). Tables 11 and 12 present pipes and nodes characteristics of this case study. The network is gravitationally fed using 3 reservoirs.

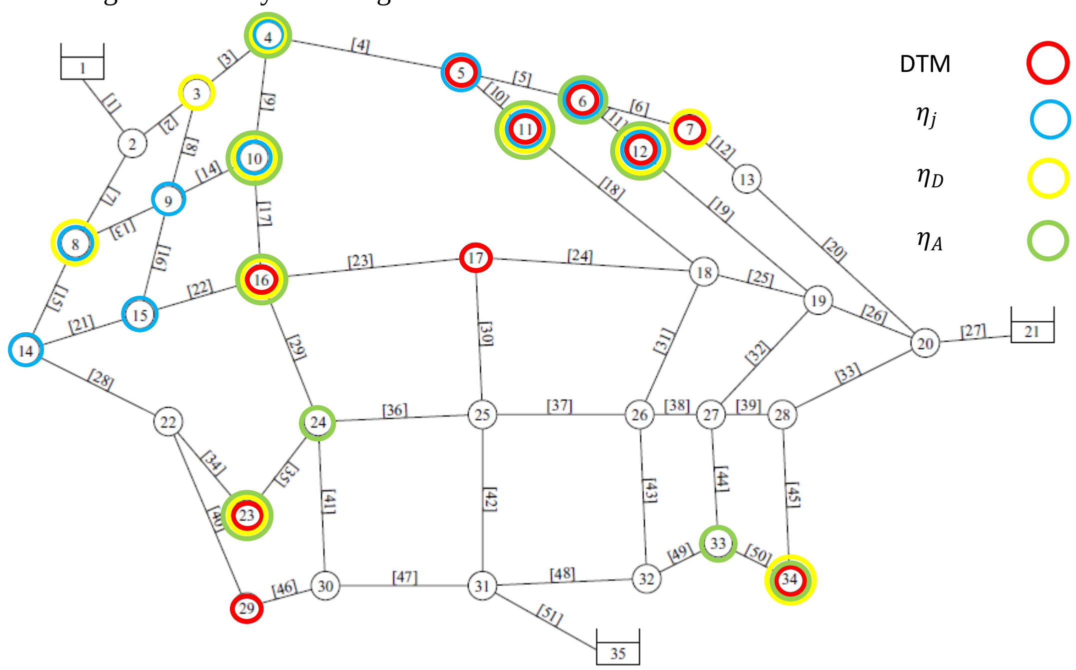


**Figure 4. Locating the measurement nodes according to DTM and $\eta_j$, $\eta_D$ *and* $\eta_A$ indices method [14] for $N_s = 10$**

The transient flow is generated by an instantaneously closing valve that discharges 0.71L/s flow to the atmosphere at node 7 at time t=1.0 s. The analysis time step is 0.01 second and the hydraulic transient simulation model is run for 4000 time steps.

Assuming that all nodes are site design candidates, the measurement site design is performed by means of DTM. Table 13 to 15 represent a comparison between results from DTM and ones from [14] according to the aforementioned indices.

The location of measurement nodes achieved by DTM and three different configurations based on $\eta_j$ , $\eta_A$, $\eta_D$ indices from [14] are illustrated in Figure 4.

**Table 11. Pipe characteristics of the Example 2 network**

| Pipe | Length (m) | *a* (m/s) | *f* | *D* (mm) | Pipe | Length (m) | *a* (m/s) | *f* | *D* (mm) |
|---|---|---|---|---|---|---|---|---|---|
| 1 | 870 | 1160 | 0.0247 | 1524 | 27 | 933.14 | 1261 | 0.04 | 914.4 |
| 2 | 450.16 | 1324 | 0.0248 | 609.6 | 28 | 887.08 | 1324 | 0.0268 | 609.6 |
| 3 | 462.06 | 1359 | 0.0274 | 457.2 | 29 | 883.35 | 1359 | 0.0298 | 457.2 |
| 4 | 894.08 | 1397 | 0.0289 | 304.8 | 30 | 900.32 | 1324 | 0.0355 | 609.6 |
| 5 | 461.01 | 1397 | 0.0338 | 304.8 | 31 | 887.08 | 1324 | 0.04 | 609.6 |
| 6 | 461.01 | 1397 | 0.04 | 304.8 | 32 | 880.11 | 1397 | 0.0393 | 304.8 |
| 7 | 463.4 | 1324 | 0.0243 | 609.6 | 33 | 900.32 | 1324 | 0.0337 | 609.6 |
| 8 | 462.06 | 1359 | 0.0276 | 457.2 | 34 | 461.01 | 1397 | 0.0345 | 304.8 |
| 9 | 461.01 | 1397 | 0.0356 | 304.8 | 35 | 461.01 | 1397 | 0.04 | 304.8 |
| 10 | 447.04 | 1397 | 0.04 | 304.8 | 36 | 908.05 | 1397 | 0.0357 | 304.8 |
| 11 | 447.04 | 1397 | 0.0198 | 304.8 | 37 | 880.11 | 1397 | 0.0308 | 304.8 |
| 12 | 462.06 | 1359 | 0.0392 | 457.2 | 38 | 447.04 | 1397 | 0.0314 | 304.8 |
| 13 | 448.47 | 1359 | 0.0298 | 457.2 | 39 | 461.01 | 1397 | 0.0352 | 304.8 |
| 14 | 448.47 | 1359 | 0.034 | 457.2 | 40 | 900.32 | 1324 | 0.0286 | 609.6 |
| 15 | 463.4 | 1324 | 0.0262 | 609.6 | 41 | 883.35 | 1359 | 0.0385 | 457.2 |
| 16 | 463.4 | 1324 | 0.0289 | 609.6 | 42 | 900.32 | 1324 | 0.0298 | 609.6 |
| 17 | 461.01 | 1397 | 0.0341 | 304.8 | 43 | 880.11 | 1397 | 0.032 | 304.8 |
| 18 | 935.99 | 1397 | 0.0357 | 304.8 | 44 | 461.01 | 1397 | 0.0313 | 304.8 |
| 19 | 908.05 | 1397 | 0.04 | 304.8 | 45 | 908.05 | 1397 | 0.0319 | 304.8 |
| 20 | 913.56 | 1324 | 0.0362 | 609.6 | 46 | 450.16 | 1324 | 0.0296 | 609.6 |
| 21 | 462.06 | 1359 | 0.0162 | 457.2 | 47 | 887.08 | 1324 | 0.0298 | 609.6 |
| 22 | 462.06 | 1359 | 0.0298 | 457.2 | 48 | 900.32 | 1324 | 0.0261 | 609.6 |
| 23 | 908.05 | 1397 | 0.034 | 304.8 | 49 | 448.47 | 1359 | 0.0269 | 457.2 |
| 24 | 935.99 | 1397 | 0.0322 | 304.8 | 50 | 448.47 | 1359 | 0.0315 | 457.2 |
| 25 | 461.01 | 1397 | 0.032 | 304.8 | 51 | 996.19 | 1261 | 0.0279 | 914.4 |
| 26 | 461.01 | 1397 | 0.04 | 304.8 | | | | | |

**Table 12. Nodal characteristics of the Example 2 network**

| Node | Elevation (m) | Consumption ($m^3/s$) | Node | Elevation (m) | Consumption ($m^3/s$) |
|---|---|---|---|---|---|
| 1 | 152.4 | Res | 19 | - | 0.08495 |
| 2 | - | - | 20 | - | - |
| 3 | - | 0.05663 | 21 | 121.9 | Res |
| 4 | - | 0.08495 | 22 | - | 0.05663 |
| 5 | - | 0.07079 | 23 | - | 0.08495 |
| 6 | - | 0.11327 | 24 | - | 0.05663 |
| 7 | - | 0.04248 | 25 | - | 0.08495 |
| 8 | - | 0.05663 | 26 | - | 0.05663 |
| 9 | - | 0.11327 | 27 | - | 0.14159 |
| 10 | - | 0.11327 | 28 | - | 0.02832 |
| 11 | - | 0.11327 | 29 | - | 0.05663 |
| 12 | - | 0.05663 | 30 | - | 0.08495 |
| 13 | - | 0.05663 | 31 | - | - |
| 14 | - | 0.08495 | 32 | - | 0.05663 |
| 15 | - | 0.11327 | 33 | - | 0.08495 |
| 16 | - | - | 34 | - | 0.08495 |
| 17 | - | 0.11327 | 35 | 91.44 | Res |
| 18 | - | - | | | |

**Table 13. Comparison of DTM results with those from [14] based on $\eta_j$ (Example 2)**

| $N_S$ | DTM | $\eta_J$ | Vitkovsky et.al 2003[14] | $\eta_J$ |
|---|---|---|---|---|
| 1 | 11 | 2.96E+04 | 11 | 2.96E+04 |
| 2 | 11,12 | 5.92E+04 | 5,11 | 5.68E+04 |
| 3 | 6,11,12 | 8.66E+04 | 5,11,12 | 8.64E+04 |
| 4 | 5,6,11,12 | 1.14E+05 | 5,6,11,12 | 1.14E+05 |
| 5 | 5,6,11,12,23 | 1.38E+05 | 4,5,6,11,12 | 1.32E+05 |
| 6 | 5,6,11,12,23,34 | 1.63E+05 | 4,5,6,10,11,12 | 1.50E+05 |
| 7 | 5,6,11,12,17,23,34 | 1.85E+05 | 4,5,6,9,10,11,12 | 1.66E+05 |
| 8 | 5,6,7,11,12,17,23,34 | 2.09E+05 | 4,5,6,9,10,11,12,15 | 1.83E+05 |
| 9 | 5,6,7,11,12,17,23,29,34 | 2.28E+05 | 4,5,6,9,10,11,12,14,15 | 1.99E+05 |
| 10 | 5,6,7,11,12,16,17,23,29,34 | 2.46E+05 | 4,5,6,8,9,10,11,12,14,15 | 2.12E+05 |

**Table 14. Comparison of DTM results with those from [14] based on $\eta_D$ (Example 2)**

| $N_S$ | DTM | $\eta_D$ | Vitkovsky et.al 2003[14] | $\eta_D$ |
|---|---|---|---|---|
| 1 | 11 | 5.07E+62 | 11 | 5.07E+62 |
| 2 | 11,12 | 4.41E+73 | 7,11 | 1.76E+72 |
| 3 | 6,11,12 | 6.18E+78 | 7,10,11 | 8.58E+76 |
| 4 | 5,6,11,12 | 2.50E+82 | 10,11,12,23 | 8.55E+82 |
| 5 | 5,6,11,12,23 | 3.22E+86 | 7,10,11,12,23 | 1.61E+86 |
| 6 | 5,6,11,12,23,34 | 1.71E+89 | 7,10,11,12,23,34 | 1.17E+89 |
| 7 | 5,6,11,12,17,23,34 | 5.69E+90 | 4,7,10,11,12,23,34 | 3.60E+90 |
| 8 | 5,6,7,11,12,17,23,34 | 3.06E+92 | 4,7,10,11,12,16,,23,34 | 5.08E+91 |
| 9 | 5,6,7,11,12,17,23,29,34 | 2.33E+93 | 4,7,8,10,11,12,16,23,34 | 1.99E+92 |
| 10 | 5,6,7,11,12,16,17,23,29,34 | 2.17E+94 | 3,4,7,8,10,11,12,16,23,34 | 7.27E+92 |

**Table 15. Comparison of DTM results with those from [14] based on $\eta_A$ (Example 2)**

| $N_S$ | DTM | $\eta_A$ | Vitkovsky et.al 2003[14] | $\eta_A$ |
|---|---|---|---|---|
| 1 | 11 | 7.03E-01 | 11 | 7.03E-01 |
| 2 | 11,12 | 3.12E-01 | 11,23 | 2.97E-01 |
| 3 | 6,11,12 | 2.13E-01 | 10,12,23 | 2.31E-01 |
| 4 | 5,6,11,12 | 1.63E-01 | 10,11,12,23 | 1.43E-01 |
| 5 | 5,6,11,12,23 | 1.14E-01 | 10,11,12,23,34 | 1.06E-01 |
| 6 | 5,6,11,12,23,34 | 9.17E-02 | 10,11,12,23,24,34 | 9.45E-02 |
| 7 | 5,6,11,12,17,23,34 | 8.15E-02 | 6,10,11,12,23,24,34 | 7.94E-02 |
| 8 | 5,6,7,11,12,17,23,34 | 7.17E-02 | 6,10,11,12,16,23,24,34 | 7.24E-02 |
| 9 | 5,6,7,11,12,17,23,29,34 | 6.69E-02 | 4,6,10,11,12,16,23,24,34 | 6.59E-02 |
| 10 | 5,6,7,11,12,16,17,23,29,34 | 6.14E-02 | 4,6,10,11,12,16,23,24,33,34 | 6.06E-02 |

## 5.Summary and Conclusion

The number and the location of the measurement sites play a major role in the accuracy and reliability of leak detection and calibration of pipe networks through the ITA. The key fact is that measurement sites with more sensitive to unknowns' variation are more representative in reflecting the impacts of leaks and pipe friction factors. Therefore, it is more likely to find the unknown parameters of leaks and calibration when the ITA objective function is developed based on the measurements in the sensitive locations. Surveying the investigations on measurement site design in the field of ITA reveals the following common issues:

- Requiring High volume of computational effort
- The necessity to define a mathematical programming and optimization algorithm
- The Lack of any initial value for $\eta_A$and $\eta_D$
- Poor scattering of the measurement sites obtained using $\eta_j$ Index
- Sensitivities with respect to leak and pipe friction factor are not from the same order

As a remedy to the above challenges, a conceptual decision-making model, the Decision Table Method, for the measurement site design of pipe networks were proposed in the present investigation. In DTM, the decision making on near optimum measurement sites is carried out based on two criteria of the maximum sensitivity of measurement sites to unknown parameters and the maximum diversity of sites with respect to different unknown parameters. The method then presented in several steps and a flowchart. Reviewing DTM steps shows that the early advantage of DTM is that it is free from the application of any optimization technique, determination of Hessian matrix, and complex calculations for matrix inversion and computation of matrix determinants. Consequently, such a reduction in the amount of required computational effort can lead to an acceleration of the measurement site design process.

The aforementioned technique was applied against two small and large example networks and the results were compared to ones extracted from methods utilizing $\eta_j$ , $\eta_A$, $\eta_D$ parameters. Comparing the DTM results with ones from $\eta_j$ , $\eta_A$, $\eta_D$ indices approach, illustrates that the results from both method are noticeably close. In measurement site design of the large networks, DTM achieved to 4, 6, 6 out of 10 nodes exactly the same as ones from other method. Additionally, considering the configuration of measurement nodes in the large network it can be concluded that DTM results shows more dispersion than ones from $\eta_j$ and $\eta_D$ parameters. This is due to the utilization of ranking in Jacobian matrix than using its absolute values. Using the absolute values of Jacobian matrix leads to concentration of nodes in the excitation point close neighborhood and consequently decreases the dispersion (Figure 4).

It is worth mentioning that, determination of the priority of sites with respect to leak and pipe friction factors performs in separate procedures in DTM and eventually, the final design suggestion is introduced via the integration of the results. Furthermore, due to the application of the Jacobian Matrix in determining the sensitivity, high priority site parameters are eliminated in order to maintain the dispersion ratio.

In conclusion, the major benefits of DTM could be stated as follows:

1. Calculation of Hessian matrix and determinant and the inverse matrix is not needed in DTM, therefore it is much more convenient to apply and is computationally fast and economic.
2. Uniquely, in case of applying DTM to large networks, the application of optimization algorithm to find the optimum measurement site configuration is not required.
3. From the table of $\eta_j$ , $\eta_A$ and $\eta_D$ values it can be inferred that as the number of measurement sites increases, the performance indices or design criteria will be improved.
4. In DTM, the priority of nodes position is determined based on the sensitivity rank of each one with respect to each decision variables rather than their numerical value. Such an attitude leads to a decrease in undesired impacts of very high or very low sensitivities in decision making and an increase in the uniformity of selected nodes distribution.

Finally, it should be noted that, although applying various sorts of measurement site design criteria may cope with roughly similar outcomes, achieving to the exactly coincident results is rarely probable and still considering the high-level engineering judgments is inevitable.

## References


1. Carrera, J. and S.P. Neuman, Estimation of Aquifer Parameters Under Transient and Steady State Conditions: 1. Maximum Likelihood Method Incorporating Prior Information. Water Resources Research, 1986. 22(2): p. 199-210.
2. Knopman, D.S. and C.I. Voss, Multiobjective sampling design for parameter estimation and model discrimination in groundwater solute transport. Water Resources Research, 1989. 25(10): p. 2245-2258.
3. Loaiciga Hugo, A., et al., Review of Ground-Water Quality Monitoring Network Design. Journal of Hydraulic Engineering, 1992. 118(1): p. 11-37.
4. Ayvaz, M.T. and A. Elçi, Identification of the optimum groundwater quality monitoring network using a genetic algorithm based optimization approach. Journal of Hydrology, 2018. 563: p. 1078-1091.
5. Luo, Q., et al., Multi-objective optimization of long-term groundwater monitoring network design using a probabilistic Pareto genetic algorithm under uncertainty. Journal of Hydrology, 2016. 534: p. 352-363.
6. Pham, H.V. and F.T.C. Tsai, Bayesian experimental design for identification of model propositions and conceptual model uncertainty reduction. Advances in Water Resources, 2015. 83: p. 148-159.
7. Jin, X., R.S. Ranjithan, and G. Mahinthakumar, A Monitoring Network Design Procedure for Three-Dimensional (3D) Groundwater Contaminant Source Identification. Environmental Forensics, 2014. 15(1): p. 78-96.
8. Dhar, A., Geostatistics-based design of regional groundwater monitoring framework. ISH Journal of Hydraulic Engineering, 2013. 19(2): p. 80-87.
9. Babbar-Sebens, M. and B.S. Minsker, Interactive Genetic Algorithm with Mixed Initiative Interaction for multi-criteria ground water monitoring design. Applied Soft Computing, 2012. 12(1): p. 182-195.
10. Kollat, J.B., P.M. Reed, and R.M. Maxwell, Many-objective groundwater monitoring network design using bias-aware ensemble Kalman filtering, evolutionary optimization, and visual analytics. 2011. 47(2).
11. Dole-Oliver, M.-J., et al., Towards an optimal sampling strategy to assess groundwater biodiversity: comparison across six European regions. 2009. 54(4): p. 777-796.
12. Li, Y. and A.B. Chan Hilton, Optimal groundwater monitoring design using an ant colony optimization paradigm. Environmental Modelling & Software, 2007. 22(1): p. 110-116.
13. Wu, J., C. Zheng, and C.C. Chien, Cost-effective sampling network design for contaminant plume monitoring under general hydrogeological conditions. Journal of Contaminant Hydrology, 2005. 77(1): p. 41-65.
14. Vitkovsky, J.P., et al., Optimal Measurement Site Locations for Inverse Transient Analysis in Pipe Networks. Journal of Water Resources Planning and Management, 2003. 129(6): p. 480-492.

15. Liggett, J.A. and L.C. Chen, Inverse Transient Analysis in Pipe Networks. Journal of Hydraulic Engineering, 1994. 120(8): p. 934-955.
16. Shamloo, H. and A. Haghighi, Optimum leak detection and calibration of pipe networks by inverse transient analysis. Journal of Hydraulic Research, 2010. 48(3): p. 371-376.
17. Gamboa-Medina, M.M. and L.F.R. Reis Sampling Design for Leak Detection in Water Distribution Networks. Procedia Engineering, 2017. 186: p. 460-469.
18. Jeppson, R. W. (1976). Analysis of flow in pipe networks. Anne Arbor, Mich: Anne Arbor Science Publishers.